Journal of Neuroscience Research 78:141–150 (2004)

Glycosphingolipid Composition of Primary Cultured Human Brain Microvascular Endothelial Cells

Takashi Kanda,[1]* Toshio Ariga,[2] Hisako Kubodera,[1] Hong Lian Jin,[1] Kiyoshi Owada,[1] Takeshi Kasama,[3] Masanaga Yamawaki,[1] and Hidehiro Mizusawa[1]

[1]Department of Neurology and Neurological Science, Tokyo Medical and Dental University Graduate School, Tokyo, Japan

[2]Drug Development Technology, Eisai Co. Ltd., Tokyo, Japan

[3]Instrumental Analysis Research Center of Life Science, Tokyo Medical and Dental University Graduate School, Tokyo, Japan

Glycosphingolipid (GSL) antigens have been considered to be involved in the pathogenesis of autoimmune neurologic disorders including multiple sclerosis. To establish the GSL pattern specific for endothelial cells forming blood–brain barrier (BBB), we established a method to yield sufficient quantities of highly purified human brain microvascular endothelial cells (HBMECs) and compared their GSL composition to that of human umbilical cord vein endothelial cells (HUVECs), as the representative of endothelial cells not forming BBB. The major gangliosides were GM3 and sialyl paragloboside (LM1), and the major neutral GSLs were lactosylceramide (LacCer), globotriaosylceramide (Gb3), and globoside (Gb4). Trace amounts of GM1, GD1a, GD1b, GT1b, and sulfoglucuronosyl paragloboside (SGPG) could be detected by the high performance thin layer chromatography-overlay method. SGPG was detected only at a nonconfluent state in an amount almost 1/30 that of in nonconfluent HUVECs. Conversely, GM3 and LM1 increased significantly after confluency. The amount of Gb3 in HBMECs was almost as twice that in HUVECs. The significance of these differences in GSL content between HBMECs and HUVECs and between confluent and nonconfluent states is obscure. It might be related, however, to the defense mechanism at the BBB and to the susceptibility of the central nervous system in some disorders that target cell surface GSL, such as hemolytic uremic syndrome.

Key words: glycosphingolipid; sulfoglucuronosyl paragloboside; blood–brain barrier; human brain microvascular endothelial cell

Vascular endothelial cells (ECs) are highly versatile cells and are involved structurally as well as metabolically in various barrier functions. The characteristic features of ECs include the presence of nonthrombogenic luminal surface, expression of von Willebrand factor, prostacycline, and endothelin, and formation of a highly selective barrier to the passage of plasma constituents into the tissue parenchyma. ECs possess many structural and functional characteristics, exhibiting a wide diversity depending on the nature of the vascular bed; this property is very important for their specialized function in individual tissue and organ function (Jaffe, 1987; Kanda et al., 1994). ECs of brain microvascular origin (BMECs) are highly specialized cells believed to make up the structural basis of the blood–brain barrier (BBB). Because BMECs are the only cell groups in the nervous system that are exposed continuously to blood constituents, the information via surface receptors on BMECs are considered very important for regulation of BBB function and subsequently for homeostasis of various cations, nutrients, and growth factors in the central nervous system (CNS).

Glycosphingolipids (GSLs) are located primarily, if not exclusively, on the outer leaflet of the plasma mem-

Abbreviations: BBB, blood–brain barrier; BMEC, brain microvascular endothelial cell; BNB, blood–nerve barrier; CNS, central nervous system; DiI-Ac-LDL, 1, 1′-dioctacecyl-3,3,3′,3, tetramethyl indocarbocyanine perchlorate acetylated low-density lipoprotein; DM, Dissecting medium; EC, endothelial cell; Gb3, globotriaosylceramide; Gb4, globoside; GSL, glycosphingolipid; HBMEC, human brain microvascular endothelial cell; HPTLC, high-performance thin-layer chromatography; HUS, hemolytic uremic syndrome; HUVEC, human umbilical cord vein endothelial cell; LM1, sialyl paragloboside; LacCer, lactosylceramide; *mdr1*, multidrug resistance-1 gene; PBS, phosphate buffered-saline; PnMEC, microvascular endothelial cell of endoneurial tissue origin; PNS, peripheral nervous system; SGPG, sulfoglucuronosyl paragloboside; SIMS, matrix-assisted secondary ion mass spectrometry.

Contract grant sponsor: Ministry of Education, Science, and Culture of Japan.

*Correspondence to: Dr. Takashi Kanda, Department of Neurology and Neurological Science, Tokyo Medical and Dental University Graduate School, 1-5-45, Yushima, Bunkyo-ku, Tokyo 113-8519, Japan.
E-mail: t-kanda.nuro@tmd.ac.jp

Received 12 February 2004; Revised 25 May 2004; Accepted 1 June 2004

Published online 23 August 2004 in Wiley InterScience (www.interscience.wiley.com). DOI: 10.1002/jnr.20228

brane. GSLs, including gangliosides, have been implicated in various cellular functions such as cellular recognition and adhesion, communication, and modulation of immune responses (Kanda et al., 1995; Karlsson, 1995; Riboni et al., 1997). Knowledge about GSLs as surface antigens and receptors in BMECs is therefore crucial to understanding the pathogenesis of CNS disorders affecting the BBB. Because of the difficulty in primary culture and the maintenance of human BMECs (HBMECs), however, no data concerning the GSL composition in these cells has ever been published. Duvar et al. (2000) recently investigated the GSL composition of immortalized human cerebromicrovascular endothelial cells; however, because this endothelial cell line cannot exclude the influence of immortalization with SV40 T-antigen, GSL analysis of genuine primary cultured HBMECs has been awaited eagerly.

We recently developed a method to yield sufficient quantities of highly purified HBMECs for biochemical analysis, and we have determined the GSL composition of cultured HBMECs. The aim of this article is to establish the GSL pattern specific for the ECs forming BBB, compared to that of human umbilical cord vein endothelial cells (HUVECs) as the representative of ECs without BBB property.

MATERIALS AND METHODS

Culture Media for HBMECs

Dissecting medium (DM) contained Medium 199 (GIBCO BRL, Grand Island, NY) supplemented with 5% fetal bovine serum (FBS; BioWhittaker, Walkersville, MD), 20 mM sodium bicarbonate, 50 μg/ml heparin (Sigma, St. Louis, MO), 100 U/ml penicillin, 100 μg/ml streptomycin, 25 ng/ml amphotericin B (GIBCO BRL), and 20 mM *N*-(2-hydroxymethyl)-piperazine-*N'*-(2-ethanesulfonic acid) (HEPES; pH 7.2). HBMEC growth medium contained EBM-2 media (Sanko Jun-yaku, Tokyo, Japan) supplemented with 100 U/ml penicillin, 100 μg/ml streptomycin, and 25 ng/ml amphotericin B.

Isolation of HBMECs

HBMEC isolation was achieved using a modified method of Gordon et al. (1991), which was designed originally for rat capillary endothelial cells. Brain tissue was removed approximately 6 hr postmortem from a 65-year-old male who had suffered from lung cancer. The tissue was rinsed thrice with DM, and the pia mater and surface vessels were removed carefully using fine forceps. The cerebral cortex was then minced to 2–3-mm cubes, rinsed several times in DM, and homogenized using a Wheaton-Dounce Teflon homogenizer. The homogenate was dissociated further with 0.005% (wt/vol) dispase (grade 1; Roche Diagnostics, Mannheim, Germany) in DM at 37°C for 2 hr in a shaking water bath. After centrifugation (800 × *g*, 5 min) the pellet was suspended with a dextran solution (mol. wt. 70,000 Daltons; 15% wt/vol in DM; Sigma), and the whole suspension was centrifuged (4°C, 4,500 × *g* for 10 min, using a Beckman JS 13.1 swinging bucket rotor). The pellet was resuspended with the dextran solution, and centrifuged again. After two centrifugations, microvessels and some single cells including red blood cells were obtained in the pellet. Other contaminating fractions including myelin and brain parenchyma were floated. The pellet was recovered with DM and filtered through 130-μm nylon mesh (Nitex; Tetko Inc., Elmsford, NY) to remove large vessels. The filtrate was digested further using collagenase/dispase (0.035% wt/vol in 10 ml DM; Roche Diagnostics) at 37°C for 12 hr in a shaking water bath. The collagenase/dispase-treated microvessels were centrifuged (800 × *g*, 5 min), rinsed and suspended in 3.0 ml DM, and then filtered through double layers of 15-μm mesh to remove single cells, which were the largest sources of non-ECs, including astrocytes and pericytes. The unfiltered cell clusters were placed into dishes coated with type I collagen (Collaborative Biomedical Products, Bedford, MA). Cells were maintained at 37°C in an atmosphere of 5% CO_2 in a humidified incubator. The medium was changed three times a week.

After 24 hr, the first migrated ECs were observed from the edge of seeded cell clusters. When the EC colonies grew sufficiently large for cloning (usually more than 100 ECs), the medium was replaced by 0.25% pancreatin solution (GIBCO BRL). The colonies for cloning (free of contamination of non-ECs, including pericytes) were marked before pancreatin treatment. The colonies were detached as clumps of ECs, and the marked colonies were picked up using a Pasteur pipette and were dissociated briefly in 0.1% trypsin in Ca^{2+}, Mg^{2+}-free Hanks' solution for 3–4 min. Cells were seeded again on 35-mm Petri dishes coated with type I rat tail collagen. After 10–21 days, confluent HBMECs, almost free of contaminating non-ECs, were subcultured at a split ratio of 1:3–5.

Identification of HBMECs

HBMECs were identified by the following four criteria: an elongated cobblestone-like appearance; immunoreactivity to anti-von Willebrand factor antigen antibody; uptake of 1, 1'-dioctacecyl-3,3,3',3, tetramethyl indocarbocyanine perchlorate acetylated low-density lipoprotein (DiI-Ac-LDL; Biomedical Technologies Inc., Stoughton, MA) (Voyta et al., 1984); and the expression of the multidrug resistance-1 (*mdr1*) gene. To label with DiI-Ac-LDL, cells were incubated with 10 μg/ml of DiI-Ac-LDL at 37°C in HBMEC growth media for 4 hr. Cells were then washed once with probe-free media for 10 min, fixed with 4% paraformaldehyde for 30 min, and viewed under a fluorescent microscope. HBMECs incorporated the bright DiI-Ac-LDL particles into their cytoplasm. Only the lots of HBMECs with more than 98% of DiI-Ac-LDL-positive cells were used for further analysis. Contaminated cells other than endothelial cells were also evaluated using mouse anti-human antibodies against glial fibrillary acidic protein (GFAP; Sigma), α smooth muscle actin (BioGenex Laboratories, San Ramon, CA), and galactocerebroside (Sigma). Less than 1% of cells were immunoreactive with these antibodies. Expression of *mdr1* mRNA, one of the most reliable pieces of evidence of their BBB-forming endothelial cell origin, was confirmed using Takara Human 3K Chip v.3.0 (Takara, Tokyo, Japan). Absence of *mdr1* mRNA in HUVEC was also confirmed.

Isolation of Glycosphingolipids

Cultured HBMECs and HUVECs (purchased from Sanko Jun-Yaku), grown confluently or semiconfluently on 100-mm Petri dishes, were harvested by scraping from the Petri dishes,

TABLE I. Glycosphingolipid Composition of Cultured HBMECs and HUVECs†

Glycosphingolipid	HBMEC-C	HBMEC-NC	HUVEC-C	HUVEC-NC
Acidic				
GM3	1,226 ± 321	254 ± 110*	2,321 ± 166	1,226 ± 194
LM1	583 ± 103	178 ± 36**	879 ± 314	464 ± 81
GM1	7.1 ± 0.9	6.2 ± 1.6	8.5 ± 1.7	6.0 ± 0.5
GD1a	4.3 ± 0.6	3.7 ± 1.0	3.0 ± 0.9	2.6 ± 0.7
GD1b	Trace	Trace	Trace	Trace
GT1b	2.5 ± 1.0	2.7 ± 0.9	2.5 ± 0.5	1.8 ± 0.9
Neutral				
LacCer	295 ± 102	182 ± 88	368 ± 139	339 ± 54
Gb3	548 ± 131	612 ± 185	259 ± 66	269 ± 62
Gb4	1,852 ± 483	1,359 ± 383	1,195 ± 530	1,205 ± 304

†HBMEC-C, human brain microvascular endothelial cell, confluent state; HBMEC-NC, human brain microvascular endothelial cell, nonconfluent state; HUVEC-C, human umbilical cord vein endothelial cell, confluent state; HUVEC-NC, human umbilical cord vein endothelial cell, nonconfluent state. Values were expressed as ng ± SEM per mg protein; $n = 3$.
*$P < 0.05$ vs. HBMEC-C and $P < 0.01$ vs. HUVEC-C.
**$P < 0.01$ vs. HBMEC-C and $P < 0.05$ vs. HUVEC-C.

washed two times with PBS, pH 7.3, and homogenized in 0.5 ml of distilled water. *Nonconfluent* or *semiconfluent* culture denotes the condition where endothelial cell-free vacant space, more than 20% of total culture dish surface, is visible under inverted microscopy. These cells are expected to be still proliferating. *Confluent* culture denotes that the endothelial cells are tightly packed and no cell-free vacant space is recognizable under inverted microscopy. Cells within the fourth passage were used for GSL analysis. Protein concentrations were determined according to the method of Bradford (1976) using a Bio-Rad (Richmond, CA) protein assay kit and bovine serum albumin (BSA) as standard. Lipids were extracted with 5 ml of chloroform/methanol (1:1 by volume), and 5 ml of chloroform/methanol (1:2 by volume), successively. After evaporating the organic solvents under a nitrogen stream, lipids were dissolved in 0.5 ml chloroform/methanol/water (30:60:8 by volume; solvent A), and applied to a Sephadex LH-20 column (0.5 × 30 cm, 10-ml bed volume; Pharmacia Fine Chemicals), pre-equilibrated with solvent A. After the first 3 ml of effluent was discarded, the next 3 ml was collected as a GSL fraction (Yu et al., 1994). The GSL fraction was then applied to a DEAE-Sephadex A-25 column (2.0-ml bed volume; Pharmacia Fine Chemicals). The neutral GSL fraction was eluted with 20 ml of solvent A, and the acidic GSL fraction was eluted with 20 ml of chloroform/methanol/0.8 M sodium acetate (30:60:8 by volume; solvent B) (Yu et al., 1994). The acidic lipid fraction was evaporated to dryness and the residue was dissolved in 0.5 ml of solvent A, and then desalted by Sephadex LH-20 column as described above. The recovered gangliosides and sulfoglucuronosyl paragloboside (SGPG) were developed on a high-performance thin-layer chromatographic plate (HPTLC; Merck, Darmstadt, Germany) with the solvent system of chloroform/methanol/water containing 0.22% $CaCl_2 \cdot 2H_2O$ (55:45:10 by volume; solvent system I) and the bands were visualized by spraying the plate with resorcinol-HCl (Ando et al., 1978; Sekine et al., 1984).

The neutral GSL fraction was evaporated to dryness and the residue was subjected to mild alkaline treatment (0.5 ml of 0.4 N NaOH in methanol) at 40°C for 2 hr or room temperature overnight to remove phospholipids according to the method of Handa (1963). The reaction mixtures were applied to a Sephadex LH-20 column to remove salts as described above. Neutral GSL composition was examined by HPTLC. Before chromatography, the upper half of the plate was sprayed with 1% borate and the entire plate was activated for 30 min at 120°C to detect glucosyl ceramide and galactosyl ceramide. After application of the sample, the plate was developed with a solvent system of chloroform/methanol/water (65:35:5 by volume, solvent system II). Neutral GSLs were visualized by spraying with the orcinol-sulfuric acid reagent. The nomenclature of gangliosides follows the system of Svennerholm (1964).

Quantitation of GM3 (NeuAc), Sialyl Paragloboside (NeuAc-nLcOse$_4$), and Other Ganglio-*N*-Tetraosyl Gangliosides

The content of GM3 (NeuAc) and sialyl paragloboside (LM1) was determined by densitometric scanning of the chromatographic plate with comigration of authentic GM3 (NeuAc) and LM1, followed by visualizing with the resorcinol-HCl reagent (Ando et al., 1978). The structure of LM1 was confirmed immunochemically with the HPTLC-overlay method using anti-paragloboside (nLcOse$_4$) monoclonal antibody (kindly provided by Dr. Tai) after treatment with *Arthrobacter ureafaciens* neuraminidase (40 mU/ml) for 2 hr at room temperature. The amounts of ganglio-*N*-tetraosyl gangliosides other than GM3 were below the detection limit of the resorcinol-HCl reagent. The HPTLC plate was therefore developed with solvent system I and bands were incubated with *A. ureafaciens* neuraminidase (40 mU/ml) for 2 hr at room temperature and then overlaid with anti-rabbit asialo GM1 antibody (diluted 1:25) for 2 hr to detect these minor ganglio-*N*-tetraosyl species (Saito et al., 1985).

Quantitation of Neutral GSLs

The presence of Gb3 and Gb4 was confirmed using anti-Gb3 and anti-Gb4 monoclonal antibodies (kindly provided

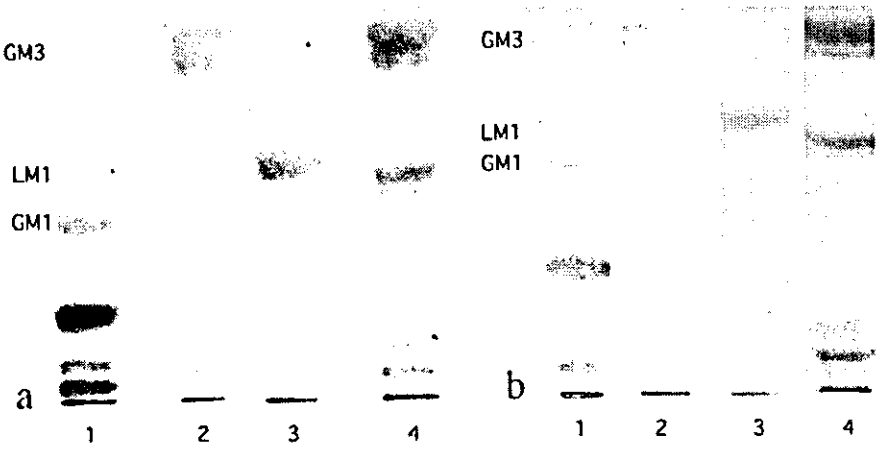

Fig. 1. Acidic glycosphingolipid (GSL) fraction in HUVECs (a) and HBMEC (b). Lane 1, human brain ganglioside standards (5 μg); lane 2, 1 μg of standard GM3 (NeuAc); lane 3, 1 μg of standard LM1; lane 4, acidic GSL fraction obtained from HUVECs (a) and HBMECs (b). The bands were visualized with the resorcinol-HCl reagent.

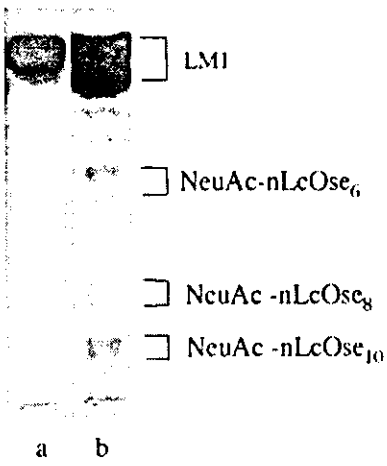

Fig. 2. a: Standard LM1 (1 μg). b: HPTLC-overlay method of acidic GSL fraction in HBMECs with the anti- nLcOse$_4$ monoclonal antibody after treatment with *A. ureafaciens* neuraminidase.

by Dr. Tai). The content of LacCer, Gb3, and Gb4 was determined by densitometric scanning of the chromatographic plate with comigration of authentic LacCer, Gb3, and Gb4, followed by visualizing with orcinol-sulfuric acid reagent.

Quantitation of SGPG (HPTLC-Overlay Method With Anti-SGPG Antibody)

Quantitative analysis of SGPG was achieved by the method described previously (Kanda et al., 1994). After the GSL fraction (collected from approximately 8–20-mg protein sample) and authentic SGPG (from 2–120 ng in quantity) were chromatographed in solvent system I, the plate was dipped in 0.4% polyisobutylmethacrylate solution in hexane for 1 min and air-dried. The plate was then incubated with LT serum (anti-SGPG antibody; immunoglobulin [Ig]M) for 2 hr, the serum from a patient with demyelinative neuropathy and IgM paraproteinemia that recognizes HNK-1 epitope, at a dilution of 1:1,000 in dilution buffer, followed by peroxidase conjugated rabbit anti-human IgM (μ-chain specific, 1:1,000; Cappel) for 2 hr. The LT serum (anti-SGPG antibody) was a generous gift from Dr. R.K. Yu (Department of Biochemistry and Molecular Biology, Institute of Molecular Medicine and Genetics, Medical College of Georgia, Augusta, GA). After washing with PBS, the plate was visualized with a Konica Immunostaining HRP 1000 (Konica, Seikagaku-kogyo, Japan). Although LT serum can react with SGPG, sulfoglucuronosyl lactosaminyl paragloboside (SGLPG) and band X (Ariga et al., 1987), only SGPG could be detected in HBMECs and HUVECs. SGPG was quantitated based on standard curves generated by densitometric scanning of known amounts of SGPG developed on the same plate.

Immunostaining of HBMECs and HUVECs With Anti-SGPG Antibody

Confluently or nonconfluently cultured HBMECs and HUVECs on collagen type I-coated glass slides were fixed with 4% paraformaldehyde for 15 min and washed with PBS at least three times. After incubation in PBS with 3% nonimmunized rabbit serum, LT serum (anti-SGPG antibody; diluted 1:100 in PBS) was applied at 4°C for 72 hr. The slides were washed three times and fluorescein isothiocyanate (FITC)-conjugated rabbit anti-human IgM (μ-chain specific, 1:1,000; Cappel) was applied for 1 hr at room temperature.

HPTLC/Matrix-Assisted Secondary Ion Mass Spectrometry

Negative secondary ion mass spectrometry (SIMS) spectra of GSLs were recorded on a Finnigan TSQ 70 quadrupole mass spectrometer in the negative ion mode equipped with a cesium ion (Cs) gun as follows. After developing GSLs on an HPTLC plate, a primuline reagent was sprayed over the plate until it is visibly wet GSLs on the plate were viewed under UV light at 380 nm. Each GSL band was marked with a colored drawing pencil while still under illumination. The plate was then immersed for 20 sec in a solvent composed of 2-propanol:methanol:0.2% aqueous $CaCl_2$ (40:20:7, vol/vol). It was then placed on another glass plate, after which a polyvinylidene difluoride (PVDF) membrane sheet and a glass microfilter sheet were

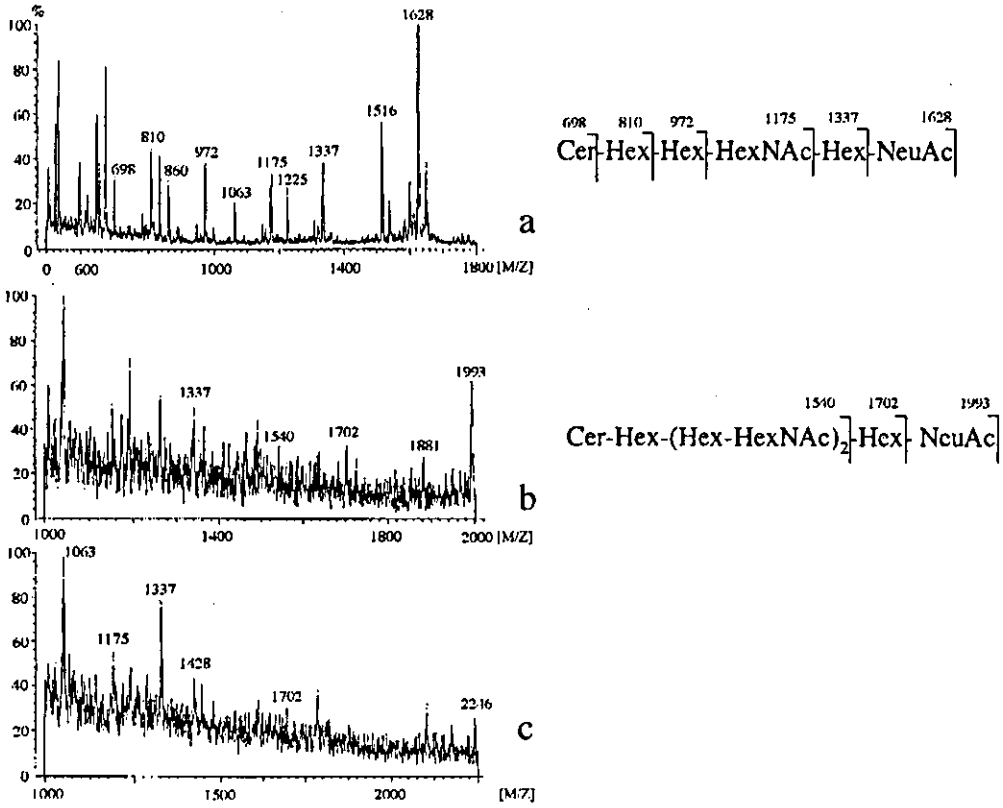

Fig. 3. Mass spectrometry of LM1 (a), NeuAc-nLcOse$_6$ (b), and NeuAc-nLcOse$_8$ (c) from HBMECs.

placed over the plate. The "sandwich" was then pressed with a household iron (about 180°C) for 30 sec. The PVDF membrane was separated from the HPTLC plate, washed with water to remove the primuline reagent, and then dried. The GSL band on the PVDF membrane was excised (2 mm in diameter) and placed on a mass spectrometer prove tip, and few microliters of triethanolamine was added as the matrix. Samples on the membrane were bombarded with a Cs^+ beam at 20 kV. The ion multiplier was kept at 1.5 kV and the conversion dynode at 20 kV (Ishikawa et al., 1995; Taki et al., 1995).

RESULTS

Glycosphingolipid composition of cultured HBMECs and HUVECs are shown in Table I.

Ganglioside Composition in HBMECs

Figure 1 shows the ganglioside pattern of the HBMECs. The two major gangliosides were identified as GM3 (NeuAc) and sialyl paragloboside (LM1; NeuAc-nLcOse$_4$) using authentic samples of GM3 (NeuAc) and LM1. LM1 was identified by HPTLC-overlay method using anti-paragloboside monoclonal antibody after neuraminidase treatment (see Fig. 2). Most bands observed in polysialoganglioside regions (Fig. 1a,b; lane 4) are neolacto-*N*-tetraose series gangliosides; it was impossible to detect ganglio-*N*-tetraose series gangliosides using resorcinol-sulfuric acid reagent (Kanda et al., 1994). In addition, this method revealed that acidic GSL fraction contained several gangliosides containing paragloboside core structures (lacto-*N*-tetraose series gangliosides; Fig. 2). The structures of these gangliosides were confirmed by HPTLC/matrix-assisted SIMS (Ishikawa et al., 1995; Taki et al., 1995) as shown in Figure 3. Negative SIMS mass spectra of gangliosides can provide information on their molecular weights and sugar sequences as well as their fatty acid and long chain base compositions. The mass spectra revealed prominent deprotonated molecules $[M - H]^-$, which corresponded to GSL molecular species containing fatty acids with chain lengths ranging from C18:0 to C24:0 and C18 sphingenine. The band comigrating to LM1 was ceramide (Cer) pentasaccharide that was found to be Cer (m/e 536-m/z 648), Cer-Hex (m/z 698-m/z 810), Cer-Hex-Hex (m/z 860-m/z 972), Cer-Hex-Hex-HexNAc (m/z 1063-m/z 1175), Cer-Hex-Hex-HexNAc-Hex (m/z 1225-m/z 1337) and Cer-Hex-Hex-HexNAc-Hex-NeuAc ($[M - H]^-$; m/z 1517-m/z 1629) (Fig. 3a). The lower band of LM1 that reacted with

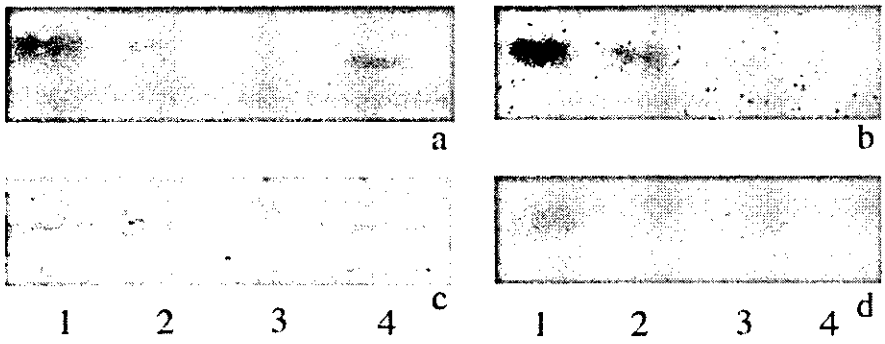

Fig. 4. HPTLC-overlay method of SGPG at a nonconfluent state in HUVECs (a) and HBMECs (c) and after confluency in HUVECs (b) and HBMECs (d). Lanes 1–3: 1.6, 0.8, and 0.4 ng of standard SGPG, respectively. Lane 4: in (a), acidic GSL fraction from 0.05 mg protein of HUVECs at nonconfluent state; in (b), acidic GSL fraction from 0.5 mg protein of HUVECs after confluency; in (c), acidic GSL fraction from 1 mg protein of HBMECs at a nonconfluent state; and in (d), acidic GSL fraction from 1 mg protein in HBMECs after confluency.

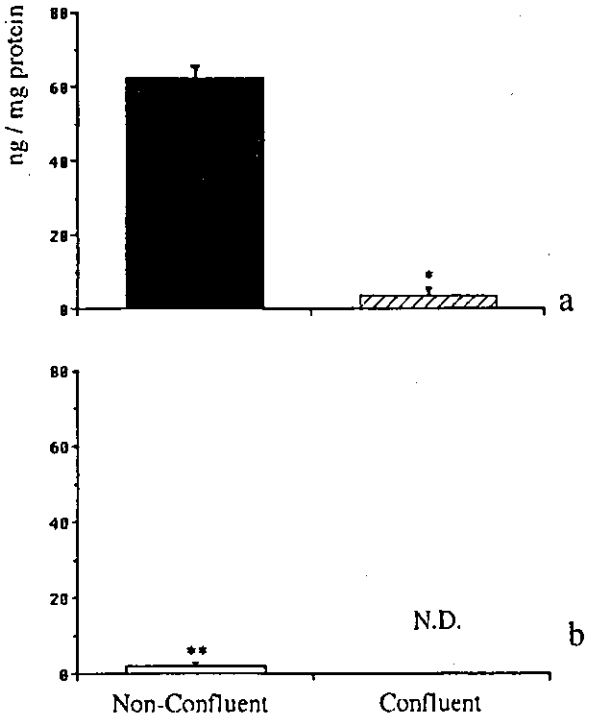

Fig. 5. SGPG content in HUVECs (a) and HBMECs (b) at nonconfluent state and after confluency. $n = 3$. Bars denote SEM. $*P < 0.0001$; $**P < 0.001$ vs. HUVECs at a nonconfluent state (black bar).

anti-paragloboside monoclonal antibody showed the deprotonated molecules (m/z 1516-m/z 1628), suggesting the presence of positional isomer of LM1 containing NeuAc (2→6) (data not shown), which the structure of NeuAc (2→6)-nLcOse$_4$ was reported by several investigators (Fukuda et al., 1985; Nojiri et al., 1988). The band that migrated to the middle position was Cer-heptasaccharide, which was found to be Cer-Hex-Hex-HexNAc-Hex (m/z 1225-m/z 1337), Cer-Hex-Hex-HexNAc-Hex-HexNAc (m/z 1428-m/z 1540), Cer-Hex-Hex-HexNAc-Hex-HexNAc-Hex (m/z 1590-m/z 1702), and Cer-Hex-Hex-HexNAc-Hex-HexNAc-Hex-NeuAc ($[M - H]^-$; m/z 1881-m/z 1993) (Fig. 3b). The second band migrated from the bottom was supposed to be Cer-nonasaccharide, but was found to be Cer-Hex-Hex-HexNAc-Hex (m/z 1225-m/z 1337), Cer-Hex-Hex-HexNAx-Hex-HexNAc (m/z 1428), Cer-Hex-Hex-HexNAc-Hex-HexNAc-Hex (m/z 1702), and Cer-Hex-Hex-HexNAc-Hex-HexNAc-Hex-HexNAc-Hex-NeuAc ($[M - H]^-$; m/z 2246) containing C18:0 fatty acid and sphingenine. Unfortunately, the deprotonated molecule at m/z 2359 containing C24:0 fatty acid and sphingenine was not detected because it was out of scales. The lower band reacted with anti-paragloboside monoclonal antibody may be ceramide containing 11 saccharides because several ions containing background ions were detected in near the deprotonated molecules (m/z 2612 - m/z 2724; data not shown). In HBMECs, GM3 and LM1 increased significantly after confluency ($P < 0.05$ and $P < 0.01$, respectively). Four ganglio-*N*-tetraosyl gangliosides, including GM1, GD1a, GD1b, and GT1b, were also detected in HUVECs and HBMECs as minor species using *A. ureafaciens* neuraminidase and anti-asialo GM1 antibody (Saito et al., 1985). No appreciable difference was noted, however, in their compositions before and after confluency.

SGPG in HBMECs and HUVECs

SGPG was found in the GSL fraction of HBMECs and HUVECs by the HPTLC-immunostaining method (Fig. 4). Neither SGLPG nor band X, found previously in human peripheral nerve (Kohriyama et al., 1987), could be detected by this method. The latter was identified as

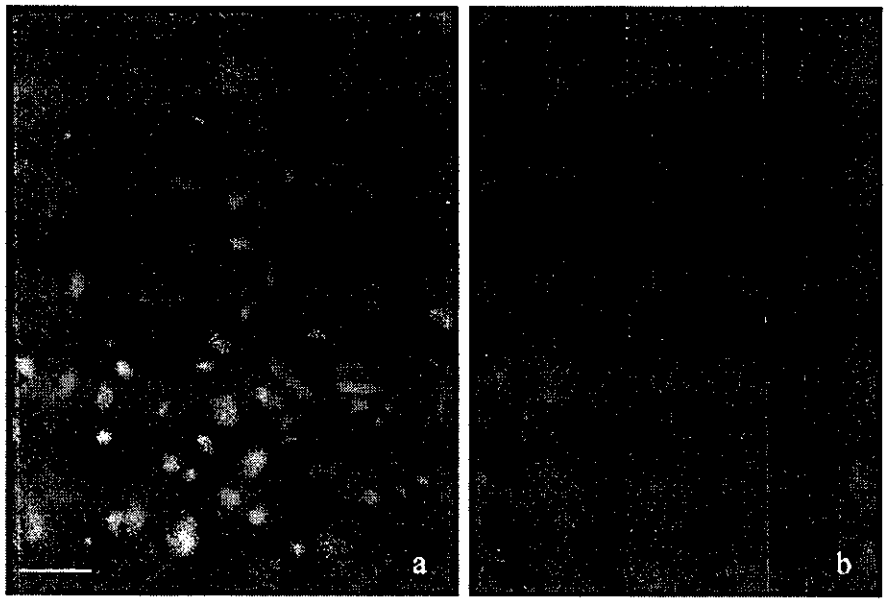

Fig. 6. Immunostaining of HUVECs before (a) and after (b) confluency using LT serum (anti-SGPG antibody). In HBMECs, no appreciable immunofluorescence was detected (data not shown). Scale bar = 100 μm.

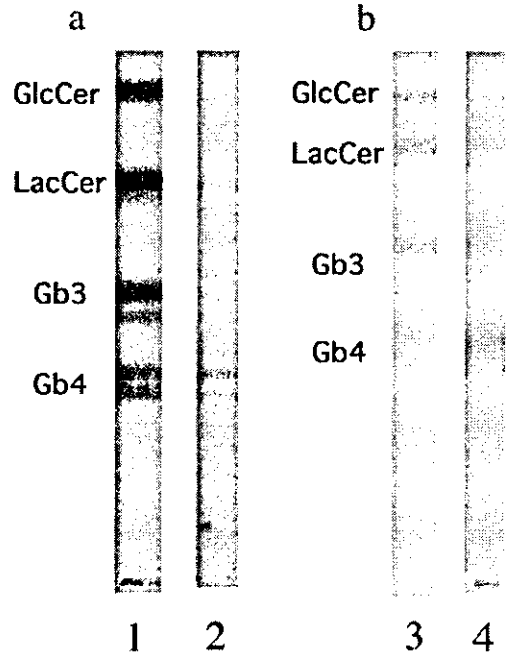

Fig. 7. Thin-layer chromatogram of neutral GSLs in HUVEC (a) and HBMEC (b). Lanes 1 and 3: 1 μg each of authentic GlcCer from human brain, LacCer, Gb3, Gb4 from porcine erythrocyte membranes (from top to bottom). Lane 2: neutral GSL fraction from HUVECs. Lane 4: neutral GSL fraction from HBMECs.

lysophosphatidylinositol (Suzuki et al., 2001). Figure 5 shows the quantitative difference of SGPG in HBMECs and HUVECs, at confluent as well as at nonconfluent culture phases. Under the nonconfluent condition, especially, when endothelial cells are in the proliferation phase and cell-to-cell contact is not conspicuous, the SGPG content in HUVECs was more than forty times as abundant as that in HBMECs. After confluency, the SGPG content in HUVECs was decreased (1/30) and no SGPG was detected in confluent HBMECs (Fig. 6).

Neutral GSL Composition of HBMECs

GSL structures were verified by immunostaining with specific anti-neutral GSL antibodies on thin-layer chromatograms. Figure 7 shows the orcinol-stained HPTLC pattern of the neutral GSL fraction in HBMECs and HUVECs, indicating these endothelial cells comprise three major neutral GSLs including LacCer, Gb3, and Gb4. The structures of these neutral GSLs were confirmed by HPTLC/SIMS (data not shown) and the HPTLC-GSL overlay method using specific antibodies (Fig. 8). Negative SIMS mass spectra of neutral GLSs showed prominent dehydrogenated molecular ions $[M - H]^-$ that corresponded to GSL molecular species containing fatty acids with chain lengths ranging from C18:0 to C24:0 and C18 sphingenine. The band comigrating to LacCer showed the fragmented ions corresponding to ceramide (Cer) (m/z 536-m/z 648), Cer-monosaccharide (m/z 698-m/z 810), and Cer-disaccharide ($[M - H]^-$; m/z 860-m/z 972), resulting in Cer-Hex-Hex. The lower two bands showed the same fragment ions corresponding to Cer, Cer-monosaccharide, and Cer-disaccharide. In the band comigrating to Gb3, the terminal sugar was found to be hexose (Hex) (m/z 162), resulting in Cer-Hex-Hex-Hex ([M -

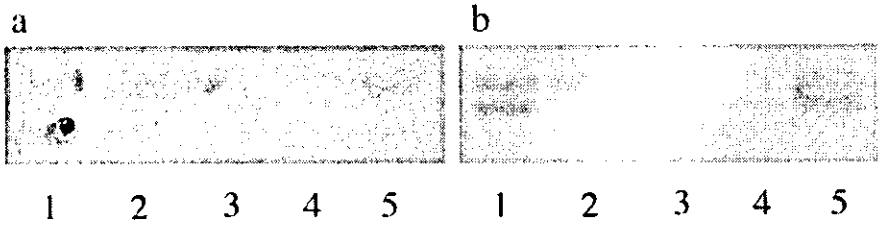

Fig. 8. HPTLC-overlay method with anti-Gb3 antibody (a) and anti-Gb4 antibody (b). Lanes 1–4: 1, .5, 0.1, 0.05 μg of authentic Gb3 (a) and Gb4 (b), respectively. Lane 5: neutral GSL fraction obtained from confluent HUVECs.

$H]^-$; m/z 1134). The band comigrating to Gb4 was Cer-tetrasaccharide and terminal sugar found to be *N*-acetylhexosamine (HexNAc) (m/z 203), resulting in Cer-Hex-Hex-Hex-HexNAc ($[M - H]^-$; m/z 1225-m/z 1337). Neither HBMECs nor HUVECs contained glucosyl ceramide or galactosyl ceramide, so far as HPTLC pattern. The amount of Gb3 in HBMECs was almost as twice that in HUVECs. No appreciable differences in neutral GSL quantity were observed before and after confluency.

DISCUSSION

It is difficult to guarantee that the cultured brain-derived ECs are really originated from ECs forming BBB. Such an assumption is made usually from elongated, fibroblast-like shape or increased resistance and limited passage of small molecules through monolayer of these cells, but conventional methods to isolate BMECs cannot escape contamination of ECs other than BMECs, namely, ECs from larger vessels lacking BBB properties. To solve this problem, we first carried out DNA microarray analysis to confirm expression of one of the most important barrier-specific genes, *mdr1* (Cordon-Cardo et al., 1989), in ECs used in the present study. Because we confirmed *mdr1* gene expression in HBMECs and its absence in HUVECs, the GSL content differences in HBMECs and HUVECs may partially reflect possible differences in cellular properties related to BBB function.

The most striking difference between GSL content of HBMECs and HUVECs is the amount of SGPG. This HNK-1 epitope-bearing GSL belongs to a novel class of acidic lipids present primarily in peripheral nerve tissues (Chou et al., 1986; Ariga et al., 1987). In mammalian CNS, sulfoglucuronosyl GSLs (SGGLs) including SGPG are known to be developmentally regulated, being expressed in embryonic forebrain and disappearing during the postnatal period (Schwarting et al., 1987), except in murine cerebellum (Chou and Jungalwala, 1988) and human optic nerve (Yoshino et al., 1993). Other than CNS parenchyma, we provided evidence that SGPG is an integral component of cultured bovine BMECs and demonstrated that SGPG is the only GSL whose concentration shows a wide fluctuation depending upon culture conditions and age (Kanda et al., 1994). Treatment of these cells with interleukin 1β (IL-1β) induced accumulation of SGPG (Kanda et al., 1995). In the present study, we found SGPG in HBMECs was much lower than that in HUVECs, and the SGPG content in both cells decreased markedly after confluency. Such marked fluctuations in SGPG expression, influenced by culture age, inflammatory cytokines, and the presence or absence of contact inhibition, may suggest a functional importance of this GSL as the surface receptor of ECs forming the BBB.

These changes in expression of SGPG may be due primarily to rapid upregulation and downregulation of glucuronyltransferase activity, probably triggered by endothelial cell–endothelial cell contact. COS-1 cells transfected with glucuronyltransferase-P cDNA (an enzyme involved in the biosynthesis of the HNK-1 epitope) (Seiki et al., 1999) and transformed into HNK-1-positive cells lost the tendency to aggregate and remained single cells (Kawasaki and Oka, 2001). The previous data and our findings indicate that the HNK-1 epitope, also known as an adhesion molecule, inhibits homophilic contact between HNK-1 epitope-bearing cells and is expressed mainly in single, proliferating cells. Because SGPG localized on BMECs acts as ligand for L-selectin expressed on the surface of circulating lymphocytes (Kanda et al., 1995) and anti-SGPG antibody (LT serum) possibly reacts with ECs forming the blood–nerve barrier and impairs their barrier function (Kanda et al., 1994, 1998), SGPG-rich proliferating ECs that repair injured barrier system may have more chance to be attacked by lymphocytes and antibodies; thus forming a vicious circle of inflammation.

The amounts of two major acidic GSLs, GM3 (NeuAc) and LM1, was also smaller in HBMECs than in HUVECs. Different from that of SGPG, the amount of GM3 (NeuAc) and LM1 was increased significantly after confluency in HBMECs. Neutral GSLs did not show any significant changes after confluency. The physiologic meaning of this difference is unknown; however, these dynamic changes in amounts of acidic GSLs including SGPG may be based on signaling systems triggered by endothelial cell–endothelial cell contact and might influence BBB integrity. The presence of neolacto-series gangliosides including NeuAc-nLcOse$_6$, NeuAc-nLcOse$_8$, and NeuAc-nLcOse$_{10}$ in HBMECs and HUVECs (Muthing et al., 1999) was confirmed using the HPTLC-overlay method and Far-Eastern blot/mass spectrometry. These minor species, however, did not show any difference between HUVECs and HBMECs.

Finally, the differences in GSL content observed in the present study and reported in previous studies are briefly discussed. HBMECs express a composition of

acidic GSLs similar to that reported previously for primary ECs from various sources (Kanda et al., 1994, 1997) and for immortalized human brain ECs (Duvar et al., 2000). The amount of acidic GSLs, however, is smaller than that observed in bovine BMECs (Kanda et al., 1994) and in immortalized human brain ECs (Duvar et al., 2000). The difference is more conspicuous in neutral GSLs: HBMEC comprise Gb4, Gb3, and LacCer as major constituents of neutral GSL whereas only GlcCer was detected in bovine BMECs (Kanda et al., 1994). These variations in expression might be attributable to species specificity and to SV40 T-antigen immortalization of ECs. Our data obtained from primary culture of nontransformed HBMECs thus should reflect more closely the in vivo GSL content of endothelial cells forming the BBB.

Species differences in neutral GSLs was also demonstrated in this study. Gb3 is known as the specific receptor for verotoxin that has been implicated strongly as the causative agent for most cases of postdiarrheal hemolytic uremic syndrome (HUS) (Lingwood, 1996) and the difference of Gb3 expression level in each organ might lead to attack of a specific organ. In this regard, preferential involvement of kidney in HUS can be well explained because verotoxin is considered to target the Gb3-rich renal microvasculature (Obrig et al., 1993) resulting in renal disorder. No reasonable explanation has ever been provided, however, for the CNS tropism in HUS. We demonstrated that the amount of Gb3 is approximately twice as abundant in HBMECs compared to that in HUVECs. This endothelial heterogeneity may explain the frequent involvement of CNS in this disorder.

ACKNOWLEDGMENT

We thank Dr. T. Tai (Department of Tumor Immunology, The Tokyo Metropolitan Institute of Medical Science) for kindly providing anti-Gb3, anti-Gb4, and anti-paragloboside monoclonal antibodies.

REFERENCES

Ando S, Chang NC, Yu RK. 1978. High-performance thin-layer chromatography and densitometric determination of brain ganglioside composition of several species. Ann Biochem 89:437–450.

Ariga T, Kohriyama T, Freddo L, Latov N, Saito M, Kohn K, Ando S, Suzuki M, Hemling ME, Rinehart KL, Kusunoki S, Yu RK. 1987. Characterization of sulfate glucuronic acid containing glycolipids reacting with IgM-M proteins in patients with neuropathy. J Biol Chem 262:848–853.

Bradford MM. 1976. A rapid and sensitive method for the quantification of protein utilizing the principle of protein-dye binding. Anal Biochem 72:248–254.

Chou DK, Ilyas AA, Evans JE, Costello C, Quarles RH, Jungalwala FB. 1986. Structure of sulfated glycolipids in the nervous system reacting with HNK-1 antibody and some IgM paraprotein in neuropathy. J Biol Chem 261:11717–11725.

Chou DK, Jungalwala FB. 1988. Sulfoglucuronyl neolactoglycolipids in adult cerebellum: specific absence in murine mutants with Purkinje cell abnormality. J Neurochem 50:1655–1658.

Cordon-Cardo C, O'Brien JP, Casals D, Rittman-Grauer L, Biedler JL, Melamed MR, Bertino JR. 1989. Multidrug-resistance gene (P-glycoprotein) is expressed by endothelial cells at blood-brain barrier. Proc Natl Acad Sci USA 86:695–698.

Duvar S, Suzuki M, Muruganandam A, Yu RK. 2000. Glycosphingolpid composition of a new immortalized human cerebromicrovascular endothelial cell line. J Neurochem 75:1970–1976.

Fukuda MN, Dell A, Oates JE, Wu P, Klock JC, Fukuda M. 1985. Structures of glycosphingolipids isolated from human granulocytes. J Biol Chem 260:1067–1082.

Gordon EL, Danielsson PE, Nguyen T, Winn HR. 1991. A comparison of primary cultures of rat cerebral microvascular endothelial cells to rat aortic endothelial cells. In Vitro Cell Dev Biol 27:313–326.

Handa S. 1963. Blood group active glycolipid from human erythrocytes. Jpn J Exp Med 33:347–360.

Ishikawa D, Kato T, Handa S, Taki T. 1995. New methods using polyvinylidene difluoride membranes to detect enzymes involved in glycosphingolipid metabolism. Anal Biochem 231:13–19.

Jaffe EA. 1987. Cell biology of endothelial cells. Hum Pathol 18:234–239.

Kanda T, Iwasaki T, Yamakawa T, Ikeda K. 1997. Isolation and culture of bovine endothelial cells of endoneurial origin. J Neurosci Res 49:769–777.

Kanda T, Usui S, Beppu H, Miyamoto K, Yamawaki M, Oda M. 1998. Blood-nerve barrier in IgM paraproteinemic neuropathy: a clinicopathologic assessment. Acta Neuropathol (Berl) 95:184–192.

Kanda T, Yamawaki M, Ariga T, Yu RK. 1995. Interleukin-1 beta up-regulates the expression of sulfoglucuronosyl paragloboside, a ligand for L-selectin, in brain microvascular endothelial cells. Proc Natl Acad Sci USA 92:7897–7901.

Kanda T, Yoshino H, Ariga T, Yamawaki M, Yu RK. 1994. Glycosphingolipid antigens in cultured microvascular bovine brain endothelial cells: sulfoglucuronyl paragloboside as a target of monoclonal IgM in demyelinative neuropathy. J Cell Biol 126:235–246.

Karlsson KA. 1995. Microbial recognition of target-cell glycoconjugates. Curr Opin Struct Biol 5:622–635.

Kawasaki T, Oka S. 2001. [Roles of the HNK-1 carbohydrate epitope in the nervous system.] Nihon Shinkei Seishin Yakurigaku Zasshi 21:95–99.

Kohriyama T, Kusunoki S, Ariga T, Yoshino JE, DeVries GH, Latov N, Yu RK. 1987. Subcellular localization of sulfated glucuronic acid-containing glycolipids reacting anti myelin-associated glycoprotein antibody. J Neurochem 48:1516–1522.

Lingwood CA. 1996. Role of verotoxin receptors in pathogenesis. Trends Microbiol 4:147–153.

Muthing J, Duvar S, Heitmann D, Hanisch HG, Neumann U, Lochnit G, Geyer R, Peter-Katalinic J. 1999. Isolation and structural characterization of glycosphingolipids of in vitro propagated human umbilical vein endothelial cells. Glycobiology 9:459–468.

Nojiri H, Kitagawa S, Nakamura M, Kirito K, Enomoto Y, Saito M. 1988. Neolacto-series gangliosides induce granulocytic differentiation of human promyelocytic leukemia cell line HL-60. J Biol Chem 263:7443–7446.

Obrig TG, Louise CB, Lingwood CA, Boyd B, Barley-Maloney L, Daniel TO. 1993. Endothelial heterogeneity in Shiga toxin receptors and responses. J Biol Chem 268:15484–15488.

Riboni L, Viani P, Bassi R, Prinetti A, Tettamanti G. 1997. The role of sphingolipids in the process of signal transduction. Prog Lipid Res 36: 153–195.

Saito M, Kasai N, Yu RK. 1985. In situ immunological determination of basic carbohydrate structure of gangliosides on thin-layer plates. Anal Biochem 148:54–58.

Schwarting GA, Jungalwala FB, Chou DKH, Boyer AM, Yamamoto M. 1987. Glucuronic acid and sulfate containing glycoconjugates are temporally and spatially regulated antigens in the developing mammalian central nervous system. Dev Biol 120:65–76.

Seiki T, Oka S, Terayama K, Imiya K, Kawasaki T. 1999. Molecular cloning and expression of a second glucuronyltransferase involved in the biosynthesis of the HNK-1 carbohydrate epitope. Biochem Biophys Res Commun 255:182–187.

Sekine M, Ariga T, Miyatake T, Kuroda Y, Suzuki A, Yamakawa T. 1984. Ganglioside composition of chromaffin granule membrane in bovine adrenal medulla. J Biochem (Tokyo) 95:155–160.

Suzuki M, Suetake K, Kasama T, Ariga T, Shiina M, Kusunoki S, Yu RK. 2001. Characterization of a phospholipid antigen reacting with serum antibody in patients with peripheral neuropathies and paraproteinemia. J Neurochem 79:970–975.

Svennerholm L. 1964. The gangliosides. J Lipid Res 5:145–153.

Taki T, Ishikawa D, Handa S, Kasama T. 1995. Direct mass spectrometric analysis of glycosphingolipid transferred to a polyvinylidene difluoride membrane by thin-layer chromatography blotting. Anal Biochem 225: 24–27.

Voyta JC, Via DP, Butterfield CE, Zetter BR. 1984. Identification and isolation of endothelial cells based on their increased uptake of acetylated-low density lipoprotein. J Cell Biol 99:2034–2040.

Yoshino H, Maeda Y, King M, Cartwright MJ, Richards DW, Ariga T, Yu RK. 1993. Sulfated glucuronyl glycolipids and gangliosides in the optic nerve of humans. Neurology 43:408–411.

Yu RK, Yoshino H, Yamawaki M, Yoshino JE, Ariga T. 1994. Subcellular distribution of sulfated glucuronyl glycolipids in human peripheral motor and sensory nerves. J Biomed Sci 1:167–171.

Original

多発性硬化症におけるNKT細胞減少は長期ステロイド治療により補正される

荒木　学，三宅　幸子，山村　隆

Continuous Oral Glucocorticoid Therapy Restores the NKT Cell Frequency in Multiple Sclerosis

Manabu Araki, Sachiko Miyake and Takashi Yamamura

Abstract

CD1d-restricted NKT cells have been implicated in the immune regulation of autoimmune diseases. We previously showed that NKT cells are reduced in number in the peripheral blood of multiple sclerosis (MS). We here raise the possibility that oral continuous glucocorticoid may restore the reduced frequency in MS. Compared with healthy subjects (HS), the total frequency of NKT cells in peripheral blood was significantly reduced in the patients in remission (MS-rem). We found that the frequency of NKT cells is significantly increased in the patients being treated with prednisolone (MS-PSL), but not in patients given IFN-β (MS-IFNβ). The cytokine profile of $CD4^+$ NKT cells from MS-rem and MS-PSL were biased towards Th2. Furthermore, $CD4^-$ NKT cells from MS-PSL showed a trend for Th2 bias. These results demonstrate that glucocorticoid would correct the reduction of NKT cells in MS. The restoration appears to be beneficial with regard to cytokine balance. It is possible that therapeutic effects of glucocorticoid may partially involve the increase of NKT cells.

Key words : MS, NKT, Th2, Glucocorticoid

はじめに

NKT細胞はCD1d拘束性に糖脂質α-galactosylceramide (α-GC)を認識し[1]，ヒトではT細胞抗原受容体にinvariant Vα24 鎖を発現するリンパ球である。活性化に伴い短時間に大量のサイトカインを産生するユニークな性質を持ち，免疫制御に重要な役割を担うことが様々な実験により確認されている。I型糖尿病[2]，全身性硬化症[3]など多くの自己免疫疾患において末梢血 NKT 細胞の減少が報告されているが，その減少の意義は依然として不明である。我々は，脱髄性免疫性神経疾患である多発性硬化症(MS) において末梢血 NKT 細胞は減少し，その減少は寛解期において顕著であることを以前に報告した[4]。また，同一患者のNKT細胞数を経時的に解析したところ，再発時（増悪時）には末梢血 NKT 細胞が増加することを確認し[5]，NKT 細胞の MS 病態との関わりを推測している。以上の研究は，治療を受けていない患者において，薬剤の影響を排除した条件で解析されたものである。一方，ステロイドや免疫調節性薬剤のヒト NKT 細胞に対する影響に関するデータは少ない[6]。今回我々は，MS の患者に対して我が国ではしばしば処方されている Glucocorticoid が in vivo で NKT 細胞にどのような影響を与えるか検討した。

国立精神・神経センター神経研究所免疫研究部　Department of Immunology, National Institute of Neuroscience, National Center of Neurology and Psychiatry

方　法

MS 患者および健常者より採血し，Ficoll-Paque Plus (Amersham Pharmacia Biotech, Uppsala, Sweden) にて末梢血単核球 (peripheral blood mononuclear cell: PBMC) を分離した。PBMC 中の NKT (TCR Vα24$^+$Vβ11$^+$) 細胞頻度は FITC 標識抗 TCR Vα24 抗体，PE 標識抗 TCR Vβ11 抗体，PE-Texas Red 標識抗 CD4 抗体，PE-cyanin 5.1 標識抗 CD8 抗体 (Immunotech, Marseille, France) を用いて染色し，フローサイトメーター (Epics XL, Beckman Coulter, Miami, FL) にて測定した。フローサイトメーターのデータ解析は EXPO 32 software (Coulter) によった。その後，24 ウェルプレートに PBMC 2×10^6 個を播種し，ヒト recombinant IL-2 (40 U/ml)，ヒト recombinant IL-7 (10 ng/ml) 存在下に糖脂質 α-GC 100 ng/ml にて刺激し，培養開始 7 日目に再度 NKT 細胞頻度を測定した。さらに 3〜4 日毎に IL-2 (40 U/ml)，IL-7 (10 ng/ml) を添加し培養を継続した。培養開始 20〜30 日目に Cell sorter (EPICS ALTRA, Beckman Coulter) にて CD4$^+$Vα24$^+$Vβ11$^+$ 細胞と CD4$^-$Vα24$^+$Vβ11$^+$ 細胞に分取し，96 ウェルプレート (平底) に 3×10^5 個を播種した。この細胞を rIL-2 (20 U/ml) 存在下に，抗-CD3/ 抗-CD28 マイクロビーズ (Dynabeads CD3/CD28 T cell expander, Dynal, Oslo, Norway) にて刺激した。2 日後 (約 54 時間後) に上清を回収し，ELISA にて IL-4 と IFN-γ の定量を行なった (BD Pharmingen, San Diego, CA)。T 細胞増殖反応の測定には，[^{3}H]thymidine (ICN, Irvine, CA) 1 μCi/well を各ウエルに添加し，72 時間後に Beta-1205 counter (Pharmacia) にてその取り込みを測定した。統計学的解析は，ノンパラメトリック検定 (Mann-Whitney の U 検定) を用いた。

対　象

MS 寛解期 52 例 (無治療群 32 例，ステロイド治療群 10 例，IFN-β 治療群 10 例)，MS 増悪期 12 例，健常者 19 例を対象とした。無治療症例は最低 3ヶ月間ステロイド剤の投与を受けておらず，また，免疫抑制剤などの免疫系に影響を与える薬剤を処方されていない症例とした。ステロイド治療群は prednisolone 5〜20 mg/日を継続的に 3ヶ月以上 (急性期治療を除く) 内服中の患者とし，IFN-β 治療は 8 MIU/隔日で治療開始 3ヶ月目の患者とした。サイトカイン産生能については無作為に抽出した健常者 7 例，MS 増悪期 5 例，MS 寛解期 15 例 (無治療 7 例，ステロイド治療 8 例) について検討した。

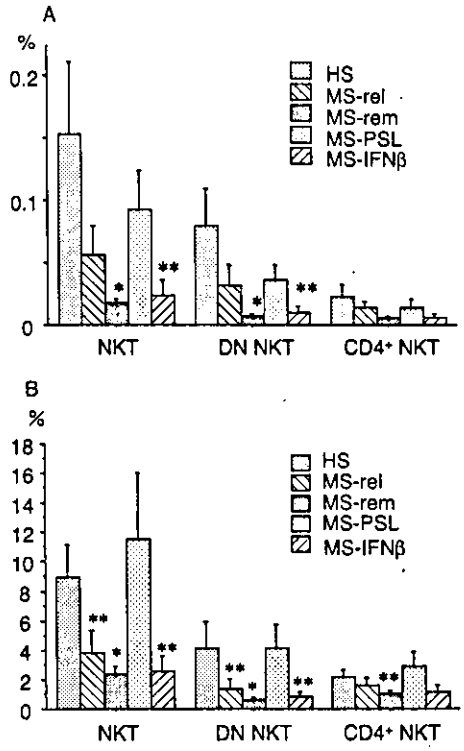

図 1　MS 患者，健常者における NKT 細胞頻度
健常者 (HS) に比較して無治療 MS 患者 (MS-rem) の末梢血 total NKT 細胞と DN NKT 細胞頻度は減少する (*$p<0.001$)．IFN-β 治療患者 (MS-IFNβ) でも同様に減少する (**$p<0.05$) 一方で，ステロイド治療患者 (MS-PSL) では減少は見られない (A)．α-GC 刺激にて NKT 細胞を増幅させた培養系における NKT 細胞頻度は，末梢血と同様，MS-rem や MS-IFNβ では健常者に比べ有意な減少を示す (MS-rem: $p<0.001$，MS-IFNβ: $p<0.05$) が，MS-PSL では減少は見られない (B)．

結　果

1) 副腎皮質ステロイド内服患者の末梢血 NKT 細胞頻度の回復

末梢血 NKT 細胞頻度は健常者に比べて MS 患者では減少し [健常者 (HS) : 0.153 ± 0.058%，MS 再発期 (MS-rel) : 0.056 ± 0.024%，MS 寛解期 (MS-rem) : 0.018 ± 0.003%]，特に寛解期において顕著であった ($p<0.001$) (図 1A)。ヒト NKT 細胞は主として CD4$^+$ NKT 細胞と CD4$^-$CD8$^-$ (double negative, DN) NKT 細胞のサブセットから構成されることから，各サブセットに分けて解析を行なったところ，DN NKT 細胞頻度は健常者に比べ有意な減少を認めた ($p<0.001$) [HS : 0.079 ± 0.017%，MS 寛解期 : 0.007 ± 0.002%]。一方，CD4$^+$ NKT 細胞は MS で減少するものの，有意差は認めなかった。今回，これ

らの無治療群（MS-rem）と比較して，ステロイド長期服用している安定期の患者（MS-PSL）（3ヶ月以上）とIFN-β治療を受け安定期にある患者（MS-IFNβ）（開始3ヶ月後）のNKT細胞頻度を調べた。その結果，MS-IFNβの末梢血NKT細胞頻度はMS-remと同じ傾向を示したのに対し（$CD4^+$ NKT細胞：$p=0.76$，DN NKT細胞：$p=0.82$=MS-remに対して），MS-PSLはMS-remに対し高値を示した（DN NKT細胞：$p<0.05$，$CD4^+$ NKT細胞：$p=0.098$=MS-remに対して）。

NKT細胞は末梢血において稀少な集団であることから，その機能解析にはNKT細胞数をin vitroにおいて増幅させる必要がある。今回はNKT細胞の糖脂質リガンドであるα-GCを用いて短期培養を行ない細胞数を増加させた。その結果，培養細胞中のNKT細胞頻度は，特定のサブセットのみが増幅することなく，末梢血NKT細胞頻度と同様の傾向を示した。HSに比べてMS-remのNKT細胞，特にDNサブセット，の著明な減少を認めた（$p<0.001$）（図1B）。MS-IFNβのNKT細胞頻度もMS-remと同様に減少を認めた（$p<0.05$）。一方，MS-PSL由来のNKT細胞培養ではMS-remに比べ有意な高値を示した（$CD4^+$ NKT細胞：$p<0.05$，DN NKT細胞：$p<0.05$，MS-remに対して）。

2）ステロイド治療患者由来NKT細胞のTh2偏倚

α-GC刺激にてin vitroで増幅させた各群（HS, MS-rel, MS-rem, MS-PSL）からNKT細胞を分離し，そのサイトカイン産生を解析した。まずcell sorterにて$CD4^+$と$CD4^-$のサブセットに分取し，各々のサブセット毎の産生量を調べた（図2）。$CD4^+$ NKT細胞については，HSに比べてMS-remのIL-4産生量が有意に高く（$p<0.01$），以前の我々の結果を再確認した。MS-PSLもHSに比べIL-4の産生量の高値を認めたが，有意差はなかった（$p=0.20$）。一方，IFN-γ産生量に関しては，各群間で有意差は認めなかった。炎症抑制的に働くIL-4と炎症性サイトカインのIFN-γの比（IL-4/IFN-γ比）を調べたところ（図3A），MS-remでは明らかな比の高値，すなわちTh2偏倚を示し（$p<0.01$，MS-relに対して），ステロイド治療群も相対的に高値を示した（$p=0.31$，MS-relに対して）。もう一つのサブセットである$CD4^-$ NKT細胞では，MS-remではIL-4, IFN-γともに産生量が減少したためにTh1/Th2偏倚は認めなかった。しかし，MS-PSLではIL-4産生量の高値を認め，IL-4/IFN-γ比ではTh2偏倚を認めた（$p=0.02$，MS-relに対し）。したがって，MS-PSLでは$CD4^+$ NKT細胞，$CD4^-$ NKT細胞ともにTh2偏倚の傾向を示し，さらにNKT細胞全体として有意差は認めないものの（$p=0.18$，MS-relに対し），Th2偏倚の傾向を示した（図3B）。MS-remでは相対的に$CD4^+$ NKT細胞が優位となりIL-4産生増加とIFN-γ産生減少が生じ，$CD4^-$ NKT細胞は著減しサイトカイン産生量が減少する。それに対

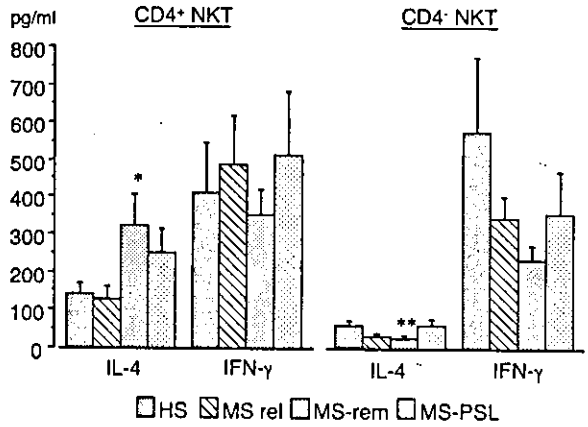

図2 $CD4^+$ NKT細胞と$CD4^-$ NKT細胞のサイトカイン産生能
MS患者，健常者由来の$CD4^+$ NKT細胞と$CD4^-$ NKT細胞を抗CD3/CD28マイクロビーズに刺激し各々のIL-4とIFN-γ産生を測定した。MS-remとMS-PSL由来の$CD4^+$ NKT細胞はHS由来のものに比べIL-4を多量に産生した。また，$CD4^-$ NKT細胞はMS-rem由来ではHSに比べて，IL-4産生が減少するのに対し，MS-PSL由来の$CD4^-$ NKT細胞はMS-remに比べてIL-4産生が増加した（$^*p<0.01$，$^{**}p<0.05$，HSに対して）。

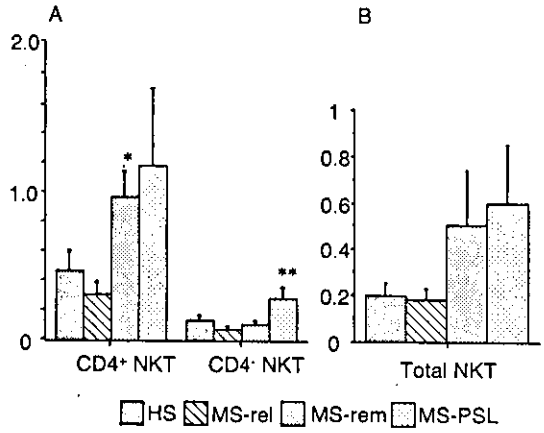

図3 MS寛解期NKT細胞のTh2偏倚
MS-remとMS-PSL由来の$CD4^+$ NKT細胞はTh2偏倚（IL-4/IFN-γ比の増大）を認めた．MS-PSL由来$CD4^-$ NKT細胞もTh2偏倚を示した（$^*p<0.01$，$^{**}p<0.05$，MS-relに対して）(A)．NKT細胞全体のサイトカイン産生はMS-remとMS-PSLにおいてTh2偏倚の傾向を示した（B)．

してMS-PSLではIL-4の産生能の低いCD4⁻NKT細胞頻度が高いものの，そのサイトカイン産生能はTh2偏倚を示すことから（図3A），NKT細胞全体としてはMS-remと同様にTh2偏倚を示した（図3B）。

考　察

invariant Vα24⁺ NKT（iNKT）細胞は短時間に大量のサイトカインを産生するユニークな免疫制御細胞である[1]。全身性硬化症患者の末梢血NKT細胞の減少が報告されて以来[3]，数多くの自己免疫疾患でその減少が報告されて来た。その減少のメカニズムの詳細は不明の部分が多いが，我々はMSにおけるNKT細胞の減少を最初に報告した[4]。さらにNKT細胞を構成するCD4⁺NKT細胞とDN NKT細胞の二つのサブセットに分けて解析し検討を加えた。CD4⁺NKT細胞はDN NKT細胞に比べIL-4を多量に産生するサブセットであるが，MS寛解期では，このCD4⁺サブセットの数が相対的に温存され，しかもIL-4のさらなる産生亢進を示すことから，NKT細胞全体としてはTh2に偏倚し病態の抑制に寄与する可能性を提唱した[5]。これらのデータは寛解期のMS患者の解析によったが，MSを含め多くの自己免疫疾患で用いられている副腎皮質ホルモン（Glucocorticoid）のNKT細胞に与える影響に関しては未知の部分が多く，今回はステロイド治療群に焦点をしぼって解析した。

Tamadaら[7]は，マウスIL-4産生NKT細胞がdexamethasone-induced apoptosisに抵抗性を示し，Th1/Th2バランスに影響を与える可能性を示唆したが，Milnerら[8]はヒトNKT細胞において同様のデータを示した。その他にも，ストレスによる内因性glucocorticoidの上昇に伴いNKT細胞がアポトーシス抵抗性を示すことも報告され[9,10]，NKT細胞とglucocorticoidの関連性が徐々に明らかになってきている。自己免疫疾患におけるglucocorticoidに対するNKT細胞の反応性について，最近Immune thrombocytopenia（ITP）患者に関する研究[6]がある。この研究では，prednisolone治療中の患者由来のNKT細胞はα-GCに対する反応性が顕著に低下することが示され，自己免疫疾患の治療におけるprednisoloneの免疫抑制にNKT細胞の介在が示唆される所見として報告されたことは興味深い。

我々は寛解再発型MSで長期ステロイド治療（最低3ヶ月）を受けている患者に焦点を当て，そのNKT細胞頻度とサイトカイン産生能を評価した。驚くべきことに，長期ステロイド治療群では，無治療寛解群に比べて，その末梢血NKT細胞頻度が有意に高値を示した。一方，IFN-β治療群と無治療寛解群との間にはNKT細胞頻度の差は認めず，NKT細胞頻度の増加はglucocorticoid特有の現象と考えられた。ただし，同一患者における無治療寛解期とステロイド長期治療期を経時的に調べることはできなかったため，このNKT細胞頻度の増加（回復）がglucocorticoidにより直接誘導されたものかどうかは不明である。一般的にMS寛解期の長期ステロイド治療には再発予防効果を期待できないとされているが，ステロイド減量に伴い症状の増悪を示すように思われる症例も存在する。IFN-β治療患者ではNKT細胞の増加を認めないことから，ステロイド長期使用がNKT細胞を増加させるものと推測される。さらに興味深いことに，ステロイド治療患者由来のNKT細胞はCD4⁺，DNサブセットともにサイトカイン産生ではTh2偏倚を示していた。glucocorticoidのMS病態抑制への関与を示唆するデータとして興味深いと考えられる。ステロイド治療を行なっていない寛解期患者（MS-rem）ではNKT細胞数は減少するものの，CD4⁺NKT細胞が相対的に温存され，しかも，各CD4⁺NKT細胞のIL-4産生能が著しく向上する。一方，ステロイド長期治療患者（MS-PSL）では，glucocorticoidによりNKT細胞の増加とCD4⁺NKT細胞とCD4⁻NKT細胞の両サブセットのTh2偏倚が誘導され，全体としてMS-remと同程度のTh2偏倚を示した。per cell basisで検討した今回の実験では，MS-rem由来とMS-PSL由来のNKT細胞の間に明らかなTh2誘導能の差は認めなかったが，MS-PSLではNKT細胞数が増加していることから，結果的に更なるTh2偏倚を誘導している可能性も考えられる。

glucocorticoidによるNKT細胞頻度の増加をin vitroで再現すべく，glucocorticoid（Dexamethasone）存在下にNKT細胞のα-GC反応性を確認する実験を行なった。結果は，健常者，MS寛解期（無治療，ステロイド治療），いずれの条件においても，glucocorticoidは用量依存性にNKT細胞のα-GC反応性を低下させた（データ未発表）。一方，サブセット別の解析では，寛解期（無治療，またはステロイド長期治療）由来のCD4⁺NKT細胞はDN NKT細胞に比べてglucocorticoidに対する抵抗性を示した（データ未発表）。これらの結果はMSにおけるNKT細胞の数的・機能的異常が後天的な因子によることを強く示唆する。

未だ多くの自己免疫疾患の急性期および慢性期治療に用いられる glucocorticoid は，活性化 T 細胞の Th1/Th2 サイトカインの産生をともに抑制するが，IL-10 産生は相対的にステロイドに抵抗性を示すため，基本的には Th2 偏倚を誘導すると考えられている[11]。しかしながら，生体内において，どの時点でどのような機序で切り替わるのかなど不明な点も多い。今回の結果より，長期ステロイド治療患者では，病態コントロールの一部に Th2 偏倚した NKT 細胞の増加を介した機序の存在も推測される。

参考文献

1) Godfrey DI, Hammond KJ, Poulton LD, Smyth MJ, Baxter AG. NKT cells: facts, functions and Fallacies. *Immunol. Today* 21: 573, 2000.
2) Wilson SB, Kent SC, Patton KT, Orban T, Jackson RA, Exley M, Porcelli S, Schatz DA, Atkinson MA, Balk SP, Strominger JL, Hafler DA. Extreme Th1 bias of invariant Vα24JαQ T cells in type 1 diabetes. *Nature* 391: 177–, 1999.
3) Sumida T, Sakamoto A, Murata H, Makino Y, Takahashi H, Yoshida S, Nishioka K, Iwamoto I, Taniguchi, M. Selective reduction of T cells bearing invariant Vα24JαQ antigen receptor in patients with systemic sclerosis. *J. Exp. Med.* 182: 1163–, 1995.
4) Illes Z, Kondo T, Newcombe J, Oka N, Tabira T, Yamamura T. Differential expression of NK T cells Vα24JαQ invariant TCR chain in the lesions of multiple sclerosis and chronic inflammatory demyelinating polyneuropathy. *J. Immunol.* 164: 4375–, 2000.
5) Araki M, Kondo T, Gumperz JE, Brenner MB, Miyake S, Yamamura T. Th2 bias of $CD4^+$ NKT cells derived from multiple sclerosis in remission. *Int. Immunol.* 15: 279–288, 2003.
6) Johansson U, Macey MG, Kenny D, Provan D, Newland AC. α-Galactosylceramide-driven expansion of human natural killer T cells is inhibited by prednisolone treatment. *Brit. J. Haematol.* 125: 400–404, 2004.
7) Tamada K, Harada M, Abe K, Li T, Nomoto K. IL-4-producing $NK1.1^+$ T cells are resistant to glucocorticoid-induced apoptosis: Implications for the Th1/Th2 balance. *J. Immunol.* 161: 1239–1247, 1998.
8) Milner JD, Kent SC, Ashley TA, Wilson SB, Strominger JL, Hafler DA. Differential responses of invariant Vα24JαQ T cells and MHC class II-restricted $CD4^+$ T cells to dexamethasone. *J. Immunol.* 163: 2522–2529, 1999.
9) Shimizu T, Kawamura T, Miyaji C, Oya H, Bannai M, Yamamoto S, Weerasinghe A, Halder RC, Watanabe H, Hatakeyama K, Abo, T. Resistance of extrathymic T cells to stress and the role of endogenous glucocorticoids in stress associated immuno suppression. *Scand. J. Immunol.* 51: 285–292, 2000.
10) Oya H, Kawamura T, Shimizu T, Bannai M, Kawamura H, Minagawa M, Watanabe H, Hatakeyama K, Abo T. The differential effect of stress on natural killer T (NKT) and NK cell function. *Clin. Exp. Immunol.* 121: 384–390, 2000.
11) Ashwell JD, Lu FWM, Vacchio MS. Glucocorticoids in T cell development and function. *Annu. Rev. Immunol.* 18: 309–345, 2000.

要　旨

CD1d 拘束性 NKT 細胞（iNKT 細胞）は免疫制御機能を担う調節細胞であり，$CD4^+$ サブセットと $CD4^-$ サブセットに分かれる。多発性硬化症（MS）の寛解期において $CD4^-$ NKT 細胞は減少する一方で，$CD4^+$ NKT 細胞には Th2 偏倚が誘導されており，これらは寛解維持を促進するような変化と捉えられている。今回我々は，ステロイド長期治療（3ヶ月以上，prednisolone 5–20 mg/日）を受けている MS 患者において，NKT 細胞の数的，機能的変化を解析した。その結果，末梢血 NKT 細胞はステロイド治療患者において無治療寛解期患者に比べ有意な増加を示し，サイトカイン産生能では Th2 偏倚を確認した。これらは MS における NKT 細胞の数的・機能的異常は後天的な因子によることを意味する。また，長期ステロイド治療による MS の病態制御の一部に，Th2 偏倚した NKT 細胞の増加を介した機序が存在する可能性がある。

キーワード：NKT 細胞，多発性硬化症，Glucocorticoid，Th2 偏倚

臨床免疫，41(1)：14-17，2004

特集I Th1/Th2バランスをめぐって

NKT細胞のリガンドとTh1/Th2バランス*

山村　隆**

Key Words：NKT cell, Th1/Th2, EAE, autoimmunity

はじめに

NK細胞のマーカーを発現するT細胞の中には，ペプチド/MHCではなく，糖脂質/CD1d分子を認識する集団が存在する．このような性質をもつのがNKT細胞と呼ばれる細胞集団で，数こそ少ないが，細胞障害活性や顕著なサイトカイン産生能などを発揮して，癌，感染，自己免疫などに関連した免疫応答で重要な役割を果たす[1)-3)]．NKT細胞を特異的に刺激する糖脂質リガンドα-ガラクトシルセラミド(α-galactosylceramide；α-GalCer)が発見されてからは，このリガンドや関連リガンドを投与することによって，癌，感染症，自己免疫疾患などの動物モデルが改善したという報告が相次いでおり，NKT細胞の研究は基礎と臨床にまたがる重要なテーマになっている．本稿では，NKT細胞のIL-4産生を介してTh2偏倚を効率よく誘導する糖脂質リガンドOCHの発見[4)]と，OCHによるTh1/Th2バランスの修飾，糖脂質リガンドの医薬としての将来性などについて解説する．

NKT細胞の特徴

NKT細胞の定義は研究者によって若干異なるが，ここで取り上げるのはCD1d分子に結合したα-GalCerを認識し，かつインバリアントTCRα鎖(マウスではVα14-Jα18，ヒトではVα24-Jα18)を発現する細胞である[1)3)]．α-GalCerは海綿の成分の中から最初に発見されたNKT細胞TCRのリガンドで，NKT細胞研究のツールとして広く利用されている(図1左)．TCRを架橋する抗CD3抗体やα-GalCerで刺激すると，NKT細胞は迅速に反応し，Th2サイトカイン(IL-4，IL-10，IL-13など)とTh1サイトカイン(IFN-γ)を大量に産生する．IL-4の産生はとくに迅速で，刺激が入ってから2時間で産生のピークを迎える．このような顕著なサイトカイン産生能により，NKT細胞が免疫調節に重要な役割を果たしていることは容易に推測される．Th2細胞の分化誘導に必要なIL-4はNKT細胞が産生するのではないかと議論されたことがあるが，NKT細胞のないマウスでもTh2分化が誘導できることから，この仮説は否定された．しかし，NKT細胞が免疫調節能を発揮することは多くの実験系で証明されている．重要な点は，NKT細胞には状況に応じてTh1サイトカインとTh2サイトカインの一方，または両方を産生する能力があることである(後述)．

自然界に存在するNKT細胞の糖脂質リガンド

健康個体の体内でNKT細胞が何を認識して免疫調節機能を発揮するのか，まだ明らかになっていない．NKT細胞の自然リガンド(natural ligand)はα-GalCerに構造的に類似した脂質であ

* Glycolipid ligands for NKT cells and Th1/Th2 balance.

** Takashi YAMAMURA, M.D.: 国立精神・神経センター神経研究所免疫研究部〔〒187-8502 小平市小川東町4-1-1〕; Department of Immunology, National Institute of Neuroscience, Kodaira 187-8502, JAPAN

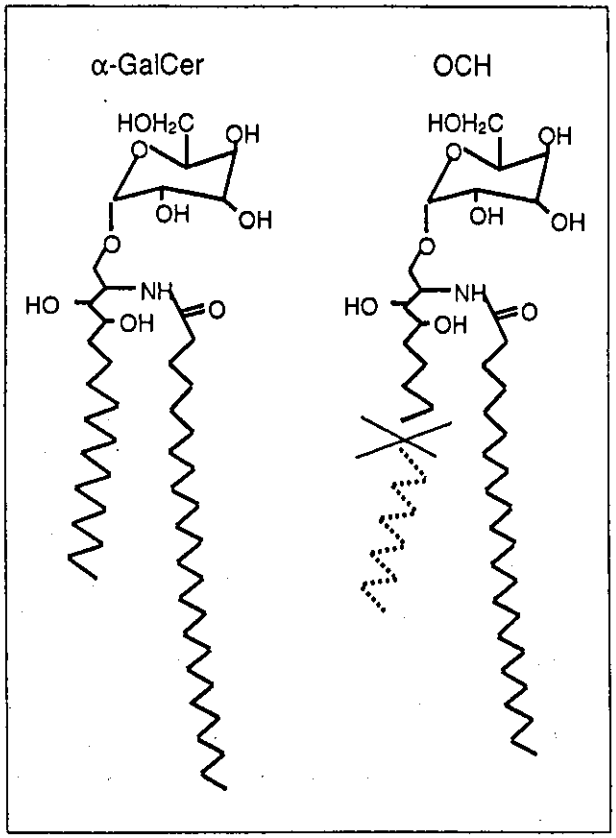

図1　α-GalCerとOCHの構造
OCHはα-GalCerの2本の疎水性炭素鎖の1本(スフィンゴシン鎖)を，炭素9個だけ短くし，もう1本のアシル鎖を炭素2個分だけ短くしたリガンドである．

ることが推測されるが，α-GalCer自体は哺乳類の生体内には存在しない．最近になって，腫瘍細胞株に由来するガングリオシドGD3や，ある種のリン脂質がNKT細胞のリガンドとして働くことが報告された[5)6)]．しかし，これらのリガンドが自然リガンドとして免疫制御に関与しているという証拠はない．なお，glycosyl phosphatidylinositols(GPI)が自然リガンドであるという報告もあるが，定説にはなっていない．

NKT細胞リガンドによる自己免疫病モデルの抑制

NKT細胞はTh2サイトカインを産生するので，糖脂質で刺激すればNKT細胞の調節機能が高まり，Th1細胞を介する自己免疫疾患が治療できるかもしれない．このような発想に基づき，われわれは代表的な自己免疫動物モデルである実験的自己免疫性脳脊髄炎(experimental autoimmune encephalomyelitis；EAE)を利用して，α-GalCer

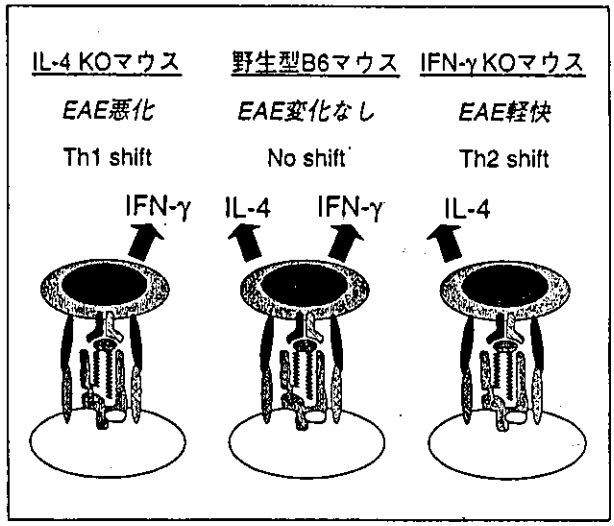

図2　α-GalCerによるEAE修飾実験の結果
α-GalCerは野生型マウスのEAEには影響を与えないが，IL-4 KOマウスのEAEは悪化させ，IFN-γ KOマウスのEAEは軽快させた．この結果は，NKT細胞の産生するIL-4とIFN-γのバランスがEAEの病態に大きな影響を与えることを意味する．

による治療実験を行った[7)]．EAEは中枢神経抗原ペプチド感作によって実験動物に誘導できる自己免疫病で，EAEを発症したマウスは中枢神経系の炎症病変とそれに伴う神経症状(後肢麻痺，失禁など)を呈する．EAEはペプチド特異的なTh1細胞移入によっても誘導が可能で，Th1細胞の関与することが確立したよいモデルである[8)]．われわれはB6マウスにEAEを誘導し，α-GalCerを腹腔内投与して治療効果を検討したが，期待に反してEAEは軽快も増悪もしなかった．さらに実験を進めた結果，α-GalCerはIL-4ノックアウトマウス(IL-4 KO)に誘導したEAEは悪化させるが，IFN-γ KOに誘導したEAEは抑制することがわかった(図2)．一連の解析結果から，α-GalCerに反応してNKT細胞の産生するIL-4はEAE抑制的に働くが，同時に産生されるIFN-γは疾患促進的であり，結果的に野生型マウスではα-GalCerの投与効果が現れないものと解釈された．

変換糖脂質リガンドOCH

MHC拘束性T細胞では，一部のアミノ酸を他のアミノ酸で置換したペプチドで刺激すると，まったく異なるサイトカイン産生パターンを示すことがある．このようにT細胞に異なる性格を寄与するペプチドを変換ペプチドリガンド

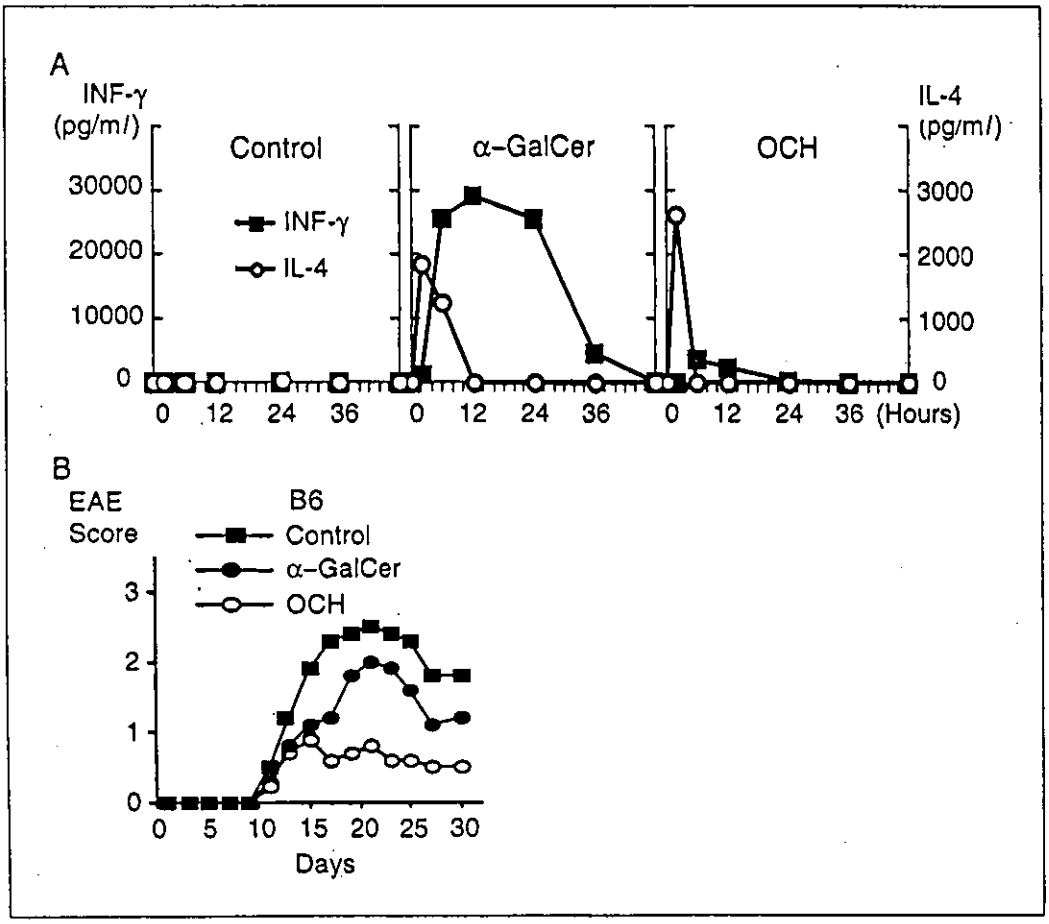

図3　α-GalCerとOCHの免疫調節活性の比較
A：腹腔内投与後の血清サイトカイン上昇パターンの違い
α-GalCerを投与したマウスではIL-4の迅速な上昇がみられ，それに引き続いてIFN-γが上昇する．一方，OCHを投与したマウスでは，IL-4の上昇はみられるが，IFN-γはほとんど検出できない．
B：EAEの治療実験
OCH経口投与によるEAE抑制を示す．縦軸はEAEの臨床スコア，横軸はEAE誘導操作後の時間経過を示す．

(altered peptide ligand；APL)と呼ぶ．このコンセプトにヒントを得て，α-GalCerの構造を一部変えたアナログの中には，NKT細胞に選択的IL-4産生を誘導するものがあるのではないかと考え，α-GalCerに修飾を加えたアナログを複数合成した．その中で，α-GalCerの疎水性炭素鎖を短縮した化合物OCH(図1)は*in vitro*でNKT細胞の選択的なIL-4産生を誘導した．また，OCHを腹腔内投与されたマウスでは，血清中のIL-4がすみやかに上昇したが，IFN-γは上昇しなかった(図3A)．野生型マウスに誘導したEAEの発症は，OCH投与によって有意に抑制され(図3B)，OCHによるNKT細胞のIL-4産生を介する可能性が考えられた．この推測は，OCHによるEAE抑制がNKT KOマウスやIL-4 KOマウスではみられないこと，OCHで治療を受けたマウスではEAEの誘導に使用したペプチド(MOG35-55)特異的T細胞がTh2偏倚していることなどの実験結果によって支持された．なお，コラーゲン誘導関節炎の発症もEAEと同じようにOCHにより抑制されるが，α-GalCerでは抑制されない[9]．これらの事実から，OCHはα-GalCerよりもTh2偏倚を誘導する能力に優れ，Th1/Th2バランスの人為的な調整を可能にする興味ある変換糖脂質リガンド(altered glycolipid ligand；AGL)であると結論づけられる．AGLがNKT細胞のサイトカイン産生プロフィルを偏倚させるメカニズムとしては，親水性部分のTCRに対するaffinityの変化，疎水性部分のCD1dに対する結合安定度の変化などを考慮する必要があり，今後の検討課題である．

おわりに

NKT細胞には作用の相反するTh1およびTh2サイトカインの両方を産生する能力があるが，そのサイトカイン産生パターンは，TCRを介する刺激の性質によって変化する．また本稿では取り上げなかったが，CD28-B7.2副刺激をブロックすることによってIL-4産生優位になることからわかるように[7]，TCR以外を介するシグナルもサイトカイン産生に影響を与える．OCHのようにTh2サイトカインの優先的な産生を誘導するリガンドは，Th1/Th2バランスをTh2に偏倚させることによってTh1自己免疫病を抑制できるので，治療薬としての発展が期待できる．

自己免疫病をTh2偏倚によって治療しようというアイデアは，多くの研究者があたためてきた．とくにAPLのコンセプトが確立してから，自己反応性T細胞をTh2に偏倚させるAPLを使った多発性硬化症治療の可能性が真剣に検討され，臨床試験まで行われた．しかし，副作用や遺伝的背景に応じて多種類のペプチドを用意しなければならないために頓挫したのが実情である．一方，糖脂質を結合するCD1d分子にはMHC分子のような多型性がなく，NKT細胞の抗原受容体も比較的均一なので，1種類のリガンドで多くの患者に均一な効果が期待できる．したがってOCHのようなAGLは，免疫バランスを人為的に修飾する薬剤として，さまざまな分野での応用が期待できる．今後ヒトのNKT細胞における解析や臨床試験を経て，AGLの実用性が検証される中で，NKT細胞と免疫調節に関する理解がさらに進むことであろう．

文　献

1) Kronenberg M, Gapin L. The unconventional lifestyle of NKT cells. Nat Rev Immunol 2002 ; 2 : 557.
2) Taniguchi M, Harada M, Kojo S, et al. The regulatory role of Vα14 NKT cells in innate and acquired immune response. Annu Rev Immunol 2003 ; 21 : 483.
3) Wilson SB, Delovitch TL. Janus-like role of regulatory iNKT cells in autoimmune disease and tumour immunity. Nat Rev Immunol 2003 ; 3 : 211.
4) Miyamoto K, Miyake S, Yamamura T. A synthetic glycolipid prevents autoimmune encephalomyelitis by inducing TH2 bias of natural killer T cells. Nature 2001 ; 413 : 531.
5) Wu DY, Segal NH, Sidobre S, et al. Cross-presentation of disialoganglioside GD3 to natural killer T cells. J Exp Med 2003 ; 198 : 173.
6) Rauch J, Gumperz J, Robinson C, et al. Structural features of the acyl chain determines self-phospholipid antigen recognition by a CD1d-restricted invariant NKT(iNKT) cells. J Biol Chem 2003 ; 278 : 47508.
7) Pál E, Tabira T, Kawano T, et al. Costimulation-dependent modulation of experimental autoimmune encephalomyelitis by ligand stimulation of Vα14 NK T cells. J Immunol 2001 ; 166 : 662.
8) 山村　隆．実験的自己免疫性脳脊髄炎．最新医学 1997 ; 52 : 1917.
9) Chiba A, Oki S, Miyamoto K, et al. Natural killer T-cell activation by OCH, a sphingosine truncated analogue of α-galactosylceramide, prevents collagen-induced arthritis. Arthritis Rheum. In press 2004.

*　　*　　*

多発性硬化症の新しい治療薬の開発

宮本勝一　山村　隆

▣ はじめに

近年，多発性硬化症 multiple sclerosis(MS)をはじめとする自己免疫疾患とナチュラルキラーT(NKT)細胞との関係が注目されている．疾患モデル動物では，NKT 細胞が自己免疫病の発症を抑制する調節機能をもつことが示され[1,2]，NKT 細胞の機能異常が MS，I 型糖尿病など，実際の自己免疫疾患の病態に関与することも推測されている[3,4]．NKT 細胞が α-ガラクトシルセラミド(α-GC)に代表される糖脂質をリガンドとして認識することが発見されて以来，種々の疾患に対して合成糖脂質を用いた治療の試みがなされている．我々は MS のモデルである実験的自己免疫性脳脊髄炎 experimental autoimmune encephalomyelitis(EAE)を用いて，NKT 細胞が EAE において調節的に働くことを明らかにしてきた[5,6]．本稿では，我々が開発した NKT 細胞を刺激する新しい合成糖脂質(OCH と命名)の投与によって EAE が抑制できることを示し，MS の新しい治療薬としての可能性を論じる．

ナチュラルキラーT(NKT)細胞の性質

NKT 細胞は，文字通り NK 細胞と T 細胞の両者の性質を併せ持つ細胞であり，多型性のない CD1d 分子により提示された糖脂質をリガンドとして認識するリンパ球である[7]．また T 細胞受容体(TCR)α 鎖が固定しているのも特徴である(マウスでは Vα 14-Jα 281 invariant 鎖，ヒトでは Vα 24-JαQ invariant 鎖)．マウスおよびヒト NKT 細胞のリガンドとして最初に発見されたのは，海綿由来の糖脂質 α-GC であるが，α-GC には転移性腫瘍を抑制する活性のあることが示されている[7]．NKT 細胞は TCR を介した刺激によって，タイプ 1 ヘルパーT 細胞(Th1)サイトカインである IFN-γ，およびタイプ 2 ヘルパーT 細胞(Th2)サイトカインである IL-4 を迅速に，かつ大量に産生する能力を持つことから，その免疫調節機能が注目されている．

NKT 細胞と多発性硬化症

今日では，MS は自己免疫疾患であり，その病態には中枢神経抗原を認識する Th1 細胞が中心的な役割を果たしていると考えられている．つまり IFN-γ や IL-2 などの Th1 サイトカインは MS の病態を増悪させる方向に働き，IL-4，IL-10 などの Th2 サイトカインは軽減させる方向に働くことになる．したがって α-GC による NKT 細胞活性化は，Th1 自己免疫病である MS に対しては IFN-γ を介して病態を増悪させる可能性と，IL-4 を介して抑制的に働く両方の可能性が考えられる．一般的に，MS 患者の NKT 細胞数は健常者に比べて減少している[3]．よって NKT 細胞が病態に関与していることが推測されるが，その中でも CD4 を発現する NKT(CD4$^+$NKT)細胞が重要であることが最近明らかになってきた．CD4$^+$NKT 細胞は，他の NKT 細胞に比べて IL-4 を主とする Th2 サイトカインの産生に重要であり，MS の病態に大きな影響を及ぼしているようである．寛解期に CD4$^+$NKT 細胞数の減少は軽度で Th2 に偏倚していることから，CD4$^+$NKT 細胞が MS の寛解維持に重要であると考えられる[8]．

リガンド活性化 NKT 細胞と実験的自己免疫性脳脊髄炎(EAE)

▣ α-GC 投与による解析

EAE は MS の動物モデルであり，主に Th1 に属する T 細胞が臓器傷害的に働くと考えられている．EAE はオリゴデンドロサイト糖蛋白(MOG)などの標的自己抗原をアジュバントとともに接種することによって誘導される．

みやもと かついち　国立精神・神経センター神経研究所/免疫研究部
やまむら たかし　同 部長

0289-0585/04/¥500/論文/JCLS